



# Perfect quantum state transfer on diamond fractal graphs

Maxim Derevyagin<sup>1</sup> · Gerald V. Dunne<sup>1,2</sup> · Gamal Mograby<sup>1</sup> ·  
Alexander Teplyaev<sup>1,2</sup> 

Received: 22 September 2019 / Accepted: 17 August 2020 / Published online: 31 August 2020  
© Springer Science+Business Media, LLC, part of Springer Nature 2020

## Abstract

In the quest for designing novel protocols for quantum information and quantum computation, an important goal is to achieve perfect quantum state transfer for systems beyond the well-known one-dimensional cases, such as 1D spin chains. We use methods from fractal analysis and probability to find a new class of quantum spin chains on fractal-like graphs (known as diamond fractals) which support perfect quantum state transfer and which have a wide range of different Hausdorff and spectral dimensions. The resulting systems are spin networks combining Dyson hierarchical model structure with transverse permutation symmetries of varying order.

**Keywords** Quantum state transfer · Quantum computer · Spin chain · Hierarchical graphs · Diamond fractal · Hamiltonians with engineered couplings · Quantum channels

## 1 Introduction

The study of state transfer was initiated by Bose [1,2], who considered a 1D chain of  $N$  qubits coupled by the time-independent Hamiltonian. The main idea is to transport a quantum state from one end of the chain to the other. The transport of the quantum state from one location to another is called perfect if it is realized with probability 1, that

---

✉ Alexander Teplyaev  
alexander.teplyaev@uconn.edu

Maxim Derevyagin  
maksym.derevyagin@uconn.edu

Gerald V. Dunne  
gerald.dunne@uconn.edu

Gamal Mograby  
gamal.mograby@uconn.edu

<sup>1</sup> Mathematics Department, University of Connecticut, Storrs, CT 06269, USA

<sup>2</sup> Physics Department, University of Connecticut, Storrs, CT 06269, USA

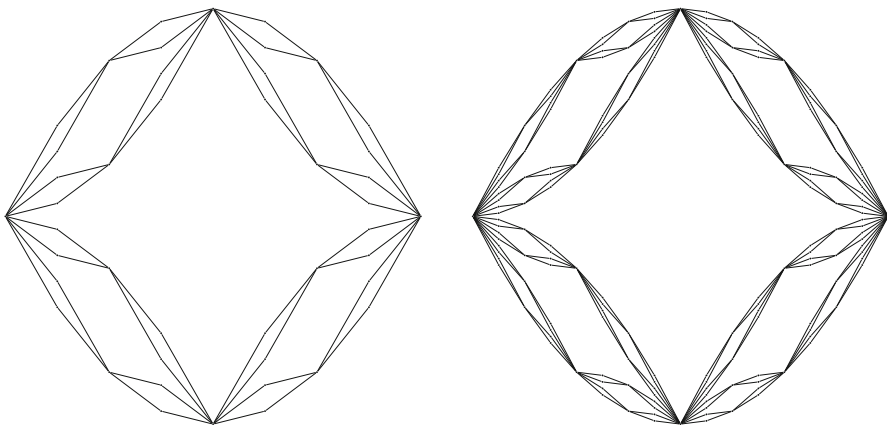


**Fig. 1** Most standard diamond hierarchical fractal graphs, levels 3 and 4, with the similarity dimension  $\dim = 2$ , [35, Section 7] and [20–30]

is, without dissipation. In addition to its fundamental interest, this means that perfect quantum state transfer also has potential applications to the design of sub-protocols for quantum information and quantum computation [3–5]. A number of one-dimensional cases, when perfect transmission can be achieved, have been found in some  $XX$  chains with inhomogeneous couplings, see [2,3,6–16, and references therein]. These models have the advantage that the perfect transfer can be done without the need for active control. Recently, there has been active interest to generalize these results to graphs with potentials and to graphs that are not one dimension [5,17–19]. These works illustrate the fact that perfect state transfer is a rare phenomenon, for which the construction of explicit examples remains rather non-trivial.

The main result of our paper is to show that perfect quantum state transfer is possible on the large and diverse class of fractal-type diamond graphs, which have different geometrical properties including a wide range of dimensions. These graphs have provided an important collection of structures with interesting physical and mathematical properties and a broad variety of geometries, see [20–32] and Figs. 1, 2, 3. The structure of these graphs is such that they combine spectral properties of Dyson hierarchical models and transport properties of one-dimensional chains. The methods that we use are discretized versions of the methods recently developed in [28,29] (see also [33,34]), which provides a construction of Green's functions for diamond fractals. Our work is part of a long-term study of mathematical physics on fractals and self-similar graphs [24,35–45], in which novel features of quantum processes on fractals can be associated with the unusual spectral and geometric properties of fractals compared to regular graphs and smooth manifolds.

## 2 1D chains

We begin with a brief summary of perfect quantum state transfer on 1D chains [3]. Consider one-dimensional Hamiltonians  $\mathbf{H}$  of the  $XX$  type with nearest neighbor

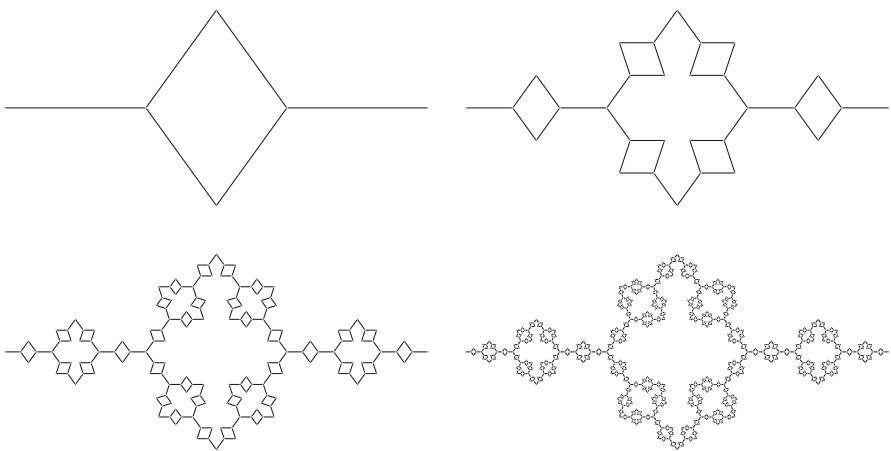


**Fig. 2** Diamond graphs of level 1, 2, 3 and 4 with uniformly bounded degree and the similarity dimension  $\dim = \frac{\log 6}{\log 4}$ , [23,31,46,47]

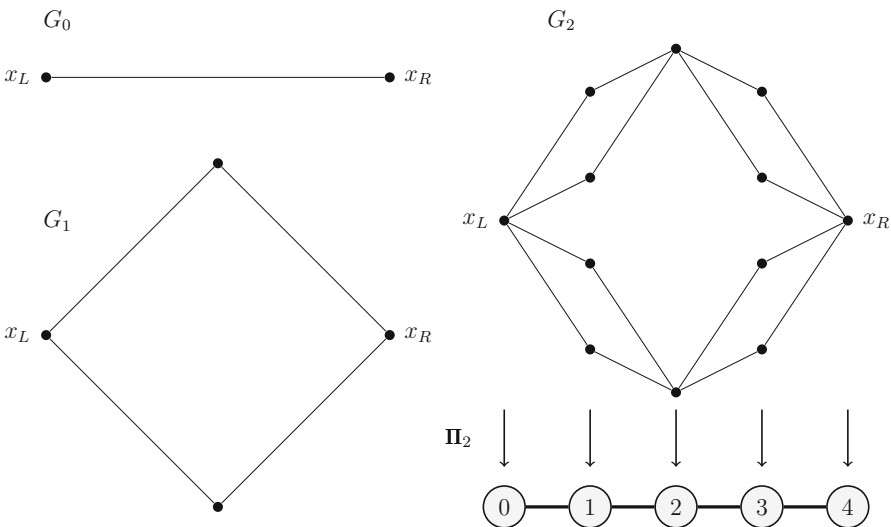


**Fig. 3** Construction of the first three levels  $G_0$ ,  $G_1$ ,  $G_2$  and the mapping  $\Pi_2$

interactions

$$\mathbf{H} = \frac{1}{2} \sum_{n=0}^{N-1} J_{n+1} (\sigma_n^x \sigma_{n+1}^x + \sigma_n^y \sigma_{n+1}^y) + \frac{1}{2} \sum_{n=0}^N B_n (\sigma_n^z + 1),$$

where  $J_n$  are the constants coupling the sites  $(n-1)$  and  $n$ , and  $B_n$  are the strengths of the magnetic field at the sites  $n$  ( $n = 0, 1, \dots, N$ ). The symbols  $\sigma_n^x$ ,  $\sigma_n^y$ ,  $\sigma_n^z$  denote

the standard Pauli matrices which act as follows on the single qubit states  $|\downarrow\rangle$  and  $|\uparrow\rangle$ :

$$\begin{aligned}\sigma^x|\downarrow\rangle &= |\uparrow\rangle, & \sigma^y|\downarrow\rangle &= -i|\uparrow\rangle, & \sigma^z|\downarrow\rangle &= -|\downarrow\rangle \\ \sigma^x|\uparrow\rangle &= |\downarrow\rangle, & \sigma^y|\uparrow\rangle &= i|\downarrow\rangle, & \sigma^z|\uparrow\rangle &= |\uparrow\rangle.\end{aligned}$$

It is straightforward to see that  $[\mathbf{H}, \sum_{n=0}^N (\sigma_n^z + 1)] = 0$  and so the eigenstates of  $\mathbf{H}$  split in subspaces labeled by the number of spins over the chain that are in state  $|\uparrow\rangle$ . It suffices to restrict  $\mathbf{H}$  to the subspace spanned by the states that contain only one excitation. A natural basis for that subspace is given by the vectors  $|n\rangle = (0, 0, \dots, 1, \dots, 0)$ ,  $n = 0, 1, 2, \dots, N$ , where the only “ $\uparrow$ ” occupies the  $n$ th position. In this basis, the restriction  $\mathbf{J}$  of  $\mathbf{H}$  to the one-excitation subspace is given by the following  $(N+1) \times (N+1)$  symmetric tridiagonal matrix

$$\mathbf{J} = \begin{pmatrix} B_0 & J_1 & & & \mathbf{0} \\ J_1 & B_1 & J_2 & & \\ & & & \ddots & \\ & & J_2 & B_2 & \\ & & & \ddots & \ddots & J_N \\ \mathbf{0} & & & & J_N & B_N \end{pmatrix}. \quad (1)$$

Such matrices are called Jacobi matrices and, as usual for the theory of Jacobi matrices, we assume that  $J_n > 0$  for  $n = 1, 2, \dots, N$ . Clearly, the action of the operator  $\mathbf{J}$  on the basis vectors  $|n\rangle$  gives

$$\mathbf{J}|n\rangle = J_{n+1}|n+1\rangle + B_n|n\rangle + J_n|n-1\rangle,$$

for  $n = 0, 1, \dots, N$ , where we set  $J_0 = J_{N+1} = 0$ . Now we can see that after some time  $t$  the initial state will evolve into the state  $e^{it\mathbf{J}}|0\rangle$ . So, in order to transfer an excitation from the site  $|0\rangle$  to the site  $|N\rangle$  there should exist  $T > 0$  and  $\phi \in \mathbb{R}$  such that

$$e^{iT\mathbf{J}}|0\rangle = e^{i\phi}|N\rangle. \quad (2)$$

As was noted in [3], the latter condition immediately implies that the entries of the Jacobi matrix  $J$  satisfy the following relations

$$B_n = B_{N-n}, \quad J_n = J_{N+1-n}, \quad n = 1, 2, \dots, N,$$

which is the mirror symmetry of the matrix  $\mathbf{J}$ . This property can also be expressed in the following way

$$\mathbf{J} = \mathbf{R}\mathbf{J}\mathbf{R},$$

where the matrix  $\mathbf{R}$ , the mirror reflection matrix, is

$$\mathbf{R} = \begin{pmatrix} 0 & 0 & \dots & 0 & 1 \\ 0 & 0 & \dots & 1 & 0 \\ \vdots & \vdots & \ddots & \vdots & \vdots \\ 0 & 1 & \dots & 0 & 0 \\ 1 & 0 & \dots & 0 & 0 \end{pmatrix}.$$

Furthermore, in [3] the following necessary and sufficient conditions for state transfer in the chain corresponding to the mirror symmetric Jacobi matrix  $\mathbf{J}$  was proved: The ordered set of the eigenvalues  $\lambda_k$  of  $\mathbf{J}$  ( $\lambda_{k-1} < \lambda_k$ ) must satisfy

$$\lambda_k - \lambda_{k-1} = (2m_k + 1)\pi/T, \quad k = 1, 2, \dots, N, \quad (3)$$

where  $T$  is the state transfer time and  $m_k$  is a nonnegative integer, which can vary with  $k$ .

As an example, we can consider one of the simplest cases of spin chains with perfect state transfer discussed in [6]. To this end, let us set

$$J_n = \frac{\sqrt{n(N+1-n)}}{2}, \quad B_n = 0 \quad (4)$$

and so the underlying Jacobi matrix is mirror symmetric and it corresponds to the symmetric Krawtchouk polynomials [48]. Also, it is known that in this case we have that

$$\lambda_k = k - N/2, \quad k = 0, 1, \dots, N, \quad (5)$$

and, thus,  $\lambda_k - \lambda_{k-1} = 1$ , which means that the condition (3) is satisfied with  $T = \pi$ . As a result, the corresponding 1D spin system can realize perfect state transfer with the transfer time  $T = \pi$ . For more examples of spin chains with perfect transfer, see [3, 19] and references therein.

### 3 Hamiltonians on graphs

We extend the results mentioned above to a collection of fractal-type diamond graphs. These graphs are no longer one dimension, so they can be used to study more complex quantum systems as an extension to the 1D spin chain models. Indeed, the diamond fractals can have a wide variety of dimensions for different choices of their self-similar structure. We equip these graphs with a general Hamiltonian that encodes their geometric information and takes the fractal-type diamond graph symmetries into account. Our main result in this paper is to show that perfect state transfer on this collection of fractal-type diamond graphs can be reduced to an appropriately constructed 1D chain. We effectively separate variables into a longitudinal direction and transverse directions related to a hierarchy of permutation symmetries. This separation leads to conditions that are sufficient to both *construct* and *design* these general Hamiltonians in such a way that guarantees perfect state transfer.

The class of fractal-type diamond graphs studied in [28] is a family of graphs  $\{G_l\}_{l \geq 0}$  which is characterized by two sequences of numbers: a sequence of *branching parameters*  $\{\mathcal{N}_l\}_{l \geq 0}$  and a sequence of *segmenting numbers*  $\{\mathcal{J}_l\}_{l \geq 0}$ . Each link on the graph branches into a given number of links and is also segmented into a given number of links. See Figs. 1, 3 for some examples that illustrate this structure. These sequences generate inductively  $\{G_l\}_{l \geq 0}$  in the following sense. At level  $l$ , we construct  $G_l$  by replacing each edge from the previous level  $G_{l-1}$  by  $\mathcal{N}_l$  new branches, whereas each new branch is then segmented into  $\mathcal{J}_l$  edges that are arranged in series. For our purposes in this paper, we will initialize  $G_0$  as the one-edge graph connecting two nodes. For example, let  $\mathcal{N}_l = \mathcal{J}_l = 2$  for all levels  $l \in \mathbb{N}$  and  $G_0$  be the one-edge graph connecting a node  $x_L$  with another node  $x_R$ . A construction of the first three levels is schematized in Fig. 3. These graphs are fractal-type in the sense that the sequence  $\{G_l\}_{l \geq 0}$  approximates a limit graph which is a special diamond fractal, see Fig. 1 for higher levels [24].

Let  $V_l$  denote the set of nodes of the diamond graph  $G_l$ . We define the mapping  $\Pi_l : V_l \rightarrow \{0, \dots, N\}$  which assigns each node  $x \in V_l$  the number of edges of the shortest path from  $x$  to the node  $x_L$ . For the most standard fractal-type diamond graphs in Fig. 1, we have  $N = 2^l$ . This is not true in general; for example, for the fractal-type graph in Fig. 2 we have  $N = 4^l$ . For level 2, the mapping  $\Pi_2$  is demonstrated in Fig. 3. The set of nodes  $V_l$  is decomposed into a disjoint union of  $N+1$  intrinsically transversal layers induced by the preimages of  $\Pi_l$ , i.e.,  $V_l = \{\Pi_l^{-1}(0) \cup \Pi_l^{-1}(1) \dots \cup \Pi_l^{-1}(N)\}$ . In particular, when a node is in the transversal layer  $\Pi_l^{-1}(n)$ , then it has an intrinsic distance of  $n$  edges to the node  $x_L$ .

A quantum state on  $G_l$  is represented by a complex-valued wave function on the nodes  $V_l$ . The space of quantum states is defined by

$$L^2(G_l) = \{\psi \mid \psi : V_l \rightarrow \mathbb{C}\}$$

which is a Hilbert space equipped with the inner product

$$\langle \psi | \varphi \rangle_{G_l} = \sum_{x \in V_l} \psi(x) \overline{\varphi(x)} \mu_l(x) \quad (6)$$

where the weights are given by  $\mu_l(x) = \frac{1}{|\Pi_l^{-1}(n)|}$  for  $n = \Pi_l(x)$  and  $|\Pi_l^{-1}(n)|$  denotes the number of nodes in the transversal layer  $\Pi_l^{-1}(n)$  that contains  $x$ . This factor accounts for the transverse degeneracies due to the permutation symmetries at a given level  $l$ . We denote by  $|x\rangle$  the wave function that assigns one to the node  $x \in V_l$  and zeros elsewhere (one-excitation state on  $G_l$ ). The set of all one-excitation states  $\{|x_L\rangle, \dots, |x_R\rangle\}$  form a natural basis for  $L^2(G_l)$ .

An  $l$ -level Hamiltonian on  $G_l$  is a Hermitian operator  $\mathbf{H}_l$  acting on  $L^2(G_l)$ . To encode the geometric information of the fractal-type diamond graph  $G_l$  in the Hamiltonian, we impose the following assumptions on  $\mathbf{H}_l$ :

- *Nearest neighbor coupling*: for  $x, y \in V_l$ , let  $\langle x | \mathbf{H}_l | y \rangle_{G_l} = 0$  if  $x$  and  $y$  are not connected by an edge, i.e., the transition matrix element from the quantum state  $|y\rangle$  to  $|x\rangle$  is zero if the nodes  $y$  and  $x$  are not adjacent in  $G_l$ .

- *Symmetric coupling*: for  $x_1, y_1, x_2, y_2 \in V_l$  such that both  $x_1, y_1$  and  $x_2, y_2$  are adjacent, let

$$\langle x_1 | \mathbf{H}_l | y_1 \rangle_{G_l} = \langle x_2 | \mathbf{H}_l | y_2 \rangle_{G_l}$$

if  $\Pi_l(x_1) = \Pi_l(x_2)$  and  $\Pi_l(y_1) = \Pi_l(y_2)$ ,

i.e., the transition matrix elements are compatible with the intrinsically transversal layers of  $G_l$ .

This means that we can regard  $\{0, \dots, N\}$  as the set of nodes of a 1D chain. To reduce the perfect state transfer problem from the graph  $G_l$  to this 1D chain, we introduce the following Hilbert space  $L^2(\{0, \dots, N\}) = \{\psi \mid \psi : \{0, \dots, N\} \rightarrow \mathbb{C}\}$  equipped with the inner product

$$\langle \psi | \varphi \rangle_l = \sum_{n=0}^N \psi(n) \overline{\varphi(n)}. \quad (7)$$

Moreover, we project a wave function in  $L^2(G_l)$  to a wave function in  $L^2(\{0, \dots, N\})$  through averaging its values on the transversal layers,

$$P_l : L^2(G_l) \rightarrow L^2(\{0, \dots, N\})$$

$$\psi \mapsto P_l \psi(n) = \frac{1}{|\Pi_l^{-1}(n)|} \sum_{x \in \Pi_l^{-1}(n)} \psi(x).$$

A simple calculation using the definition of the inner products gives  $\langle P_l \psi | \varphi \rangle_l = \langle \psi | P_l^* \varphi \rangle_{G_l}$ , where the adjoint operator  $P_l^*$  of  $P_l$  is defined by

$$P_l^* : L^2(\{0, \dots, N\}) \rightarrow L^2(G_l)$$

$$\varphi \mapsto P_l^* \varphi(x) = \varphi(\Pi_l(x)).$$

## 4 Main results and proofs

The Hamiltonian  $\mathbf{H}_l$  on  $G_l$  induces an operator on the 1D chain  $\{0, \dots, N\}$  by

$$\mathbf{J}_l = P_l \mathbf{H}_l P_l^*$$

which acts on  $L^2(\{0, \dots, N\})$ , see Fig. 4. We denote the one-excitation states in  $L^2(\{0, \dots, N\})$  by  $|n\rangle$  for a node  $n \in \{0, \dots, N\}$ . Let  $\mathbf{H}_l = (H_l(x, y))_{x, y \in V_l}$  be the matrix representation of  $\mathbf{H}_l$  with respect to  $\{|x_L\rangle, \dots, |x_R\rangle\}$ . The following result relates the matrix elements of  $\mathbf{H}_l$  to  $\mathbf{J}_l$ .

**Proposition 1** *Let  $x \in V_l$ ,*

1.  $H_l(x, x) = \langle \Pi_l(x) | \mathbf{J}_l | \Pi_l(x) \rangle_l$ .

**Fig. 4** Diagram to explain the mapping between the Hamiltonian  $\mathbf{H}_l$  on the diamond fractal graph  $G_l$  and the effective Hamiltonian  $\mathbf{J}_l$  on the associated one-dimensional spin chain. The definition of  $\mathbf{J}_l = P_l \mathbf{H}_l P_l^*$ : We apply first  $P_l^*$ , then  $\mathbf{H}_l$ , and finally  $P_l$

$$\begin{array}{ccc}
 L^2(\{0, \dots, N\}) & \xrightarrow{\mathbf{J}_l} & L^2(\{0, \dots, N\}) \\
 P_l^* \downarrow & & \uparrow P_l \\
 L^2(G_l) & \xrightarrow{\mathbf{H}_l} & L^2(G_l)
 \end{array}$$

2. Let  $y \in V_l$  be adjacent to  $x$  and  $\Pi_l(y) = \Pi_l(x) \pm 1$ , then

$$H_l(x, y) = \frac{1}{\deg_{\pm}(x)} \langle \Pi_l(x) | \mathbf{J}_l | \Pi_l(x) \pm 1 \rangle_l,$$

where  $\deg_{\pm}(x)$  is defined as follows: Let  $x \in \Pi_l^{-1}(n)$  for some  $n \in \{0, \dots, N-1\}$  the mapping  $\deg_+(x)$  assigns the node  $x$  the number of edges that connect  $x$  to nodes in  $\Pi_l^{-1}(n+1)$ . Similarly,  $\deg_-(x)$  assigns the node  $x$  the number of edges that connect  $x$  to nodes in  $\Pi_l^{-1}(n-1)$ .

3. The Hamiltonian  $\mathbf{H}_l$  is self-adjoint with respect to the inner product 6 if and only if  $\mathbf{J}_l$  is self-adjoint with respect to the inner product 7.

The following result justifies the reduction in the perfect transfer problem from  $G_l$  to a 1D chain.

**Theorem 1** If the perfect state transfer on the 1D chain  $\{0, \dots, N\}$  is achieved, i.e., there exists  $T_l > 0$  such that

$$e^{iT_l \mathbf{J}_l} |0\rangle = e^{i\phi} |N\rangle$$

for some phase  $\phi$ , then the perfect state transfer on  $G_l$  is also achieved with the same time  $T_l$  and phase  $\phi$ , i.e.,

$$e^{iT_l \mathbf{H}_l} |x_L\rangle = e^{i\phi} |x_R\rangle \text{ and } e^{iT_l \mathbf{H}_l} |x_R\rangle = e^{i\phi} |x_L\rangle.$$

For the purpose of proving the main results, we introduce first the following auxiliary definitions and lemmas. We define the space of functions  $\psi \in L^2(G_l)$  that are constant on each transversal layer  $\Pi_l^{-1}(n)$  for  $n \in \{0, \dots, N\}$  and denote it by

$$L^2_{\text{sym}}(G_l) = \{\psi \mid \psi(x) = \psi(y) \text{ if } \Pi_l(x) = \Pi_l(y)\}.$$

$L^2_{\text{sym}}(G_l)$  is a subspace of  $L^2(G_l)$  and let  $\mathbf{Proj}_l : L^2(G_l) \rightarrow L^2_{\text{sym}}(G_l)$  be the projection of  $L^2(G_l)$  onto  $L^2_{\text{sym}}(G_l)$ .

**Lemma 2**  $L^2_{\text{sym}}(G_l)$  is an invariant subspace of  $L^2(G_l)$  under  $\mathbf{H}_l$ .

**Proof** Let  $\Pi_l^{-1}(n) = \{x_{n_1}, \dots, x_{n_m}\}$  for some  $n \in \{0, \dots, N\}$  and  $|\psi\rangle = |x_{n_1}\rangle + \dots + |x_{n_m}\rangle$ , i.e., for  $x \in V_l$

$$\langle x|\psi\rangle_{G_l} = \begin{cases} \frac{1}{|\Pi_l^{-1}(n)|} & \text{if } x \in \Pi_l^{-1}(n) \\ 0 & \text{otherwise} \end{cases}$$

It suffices to show that  $\mathbf{H}_l|\psi\rangle \in L^2_{\text{sym}}(G_l)$ . By the symmetric coupling assumption on  $\mathbf{H}_l$ , we set  $c_n = \langle x_{n_1}|\mathbf{H}_l|x_{n_1}\rangle_{G_l} = \dots = \langle x_{n_m}|\mathbf{H}_l|x_{n_m}\rangle_{G_l}$ . Note that any two nodes in the same transversal layer are not adjacent. Similarly, for the neighboring transversal layers, we set  $c_{n-1} = \langle x|\mathbf{H}_l|y\rangle_{G_l}$  for any adjacent nodes  $x \in \Pi_l^{-1}(n-1)$ ,  $y \in \Pi_l^{-1}(n)$  for  $n > 0$  and  $c_{n+1} = \langle x|\mathbf{H}_l|y\rangle_{G_l}$  for any adjacent nodes  $x \in \Pi_l^{-1}(n+1)$ ,  $y \in \Pi_l^{-1}(n)$  for  $n < N$ . One can easily verify the following formula,

$$\langle x|\mathbf{H}_l|\psi\rangle = \begin{cases} \deg_{+,n-1}c_{n-1} & \text{if } x \in \Pi_l^{-1}(n-1) \\ c_n & \text{if } x \in \Pi_l^{-1}(n) \\ \deg_{-,n+1}c_{n+1} & \text{if } x \in \Pi_l^{-1}(n+1) \\ 0 & \text{otherwise} \end{cases}$$

where the last case is implied by the nearest neighbor coupling assumption on  $\mathbf{H}_l$  and  $\deg_{+,n-1}$  (or  $\deg_{-,n+1}$ ) is the number of edges that connect a node in  $\Pi_l^{-1}(n-1)$  (or  $\Pi_l^{-1}(n+1)$ ) to nodes in  $\Pi_l^{-1}(n)$ .

**Lemma 3** *The range of  $P_l^*$  is  $L^2_{\text{sym}}(G_l)$ .*

**Proof** It follows by the definition of  $P_l^*$  and  $L^2_{\text{sym}}(G_l)$ .

**Corollary 4**  *$\text{Ker } P_l = (L^2_{\text{sym}}(G_l))^{\perp}$ . In particular, if  $\psi \in (L^2_{\text{sym}}(G_l))^{\perp}$ , then the sum over a transversal layer gives  $\sum_{x \in \Pi_l^{-1}(n)} \psi(x) = 0$  for  $n \in \{0, \dots, N\}$ .*

**Proof** It follows with  $\text{Ker } P_l = (\text{Range } P_l^*)^{\perp}$  and Lemma 3.

**Lemma 5** *Let  $\psi \in L^2(G_l)$  and  $x \in V_l$ , then  $P_l^* P_l \psi(x) = \mathbf{Proj}_l \psi(x)$ .*

**Proof** We decompose  $\psi = \psi_{\text{sym}} + \psi_{\text{sym}}^{\perp}$  such that  $\psi_{\text{sym}} \in L^2_{\text{sym}}(G_l)$  and  $\psi_{\text{sym}}^{\perp} \in (L^2_{\text{sym}}(G_l))^{\perp}$ . Corollary 4 implies  $P_l^* P_l \psi = P_l^* P_l \psi_{\text{sym}}$ . Let  $n \in \{0, \dots, N\}$  and  $x \in \Pi_l^{-1}(n)$ . Then,  $\psi_{\text{sym}}$  is constant on the transversal layer  $\Pi_l^{-1}(n)$  and its averaging gives  $P_l \psi_{\text{sym}}(n) = \psi_{\text{sym}}(x)$ . Hence, by the definition of  $P_l^*$ , it follows  $P_l^* P_l \psi_{\text{sym}}(x) = \psi_{\text{sym}}(x) = \mathbf{Proj}_l \psi(x)$ .

**Proof of Proposition 1** Let  $x \in \Pi_l^{-1}(n) = \{x_{n_1}, \dots, x_{n_m}\}$  for some  $n \in \{0, \dots, N\}$ . We evaluate the matrix element,

$$\langle \Pi_l(x)|\mathbf{J}_l|\Pi_l(x)\rangle_l = \langle \Pi_l(x)|P_l \mathbf{H}_l P_l^*|\Pi_l(x)\rangle_l = \langle P_l^* \Pi_l(x)|\mathbf{H}_l|P_l \Pi_l(x)\rangle_{G_l}$$

where we adopt the notation  $|P_l^* \Pi_l(x)\rangle = P_l^* |\Pi_l(x)\rangle = |x_{n_1}\rangle + \cdots + |x_{n_m}\rangle$ . The assumptions on  $\mathbf{H}_l$  imply

$$\langle \Pi_l(x) | \mathbf{J}_l | \Pi_l(x) \rangle_l = \langle x_{n_1} | \mathbf{H}_l | x_{n_1} \rangle_{G_l} + \cdots + \langle x_{n_m} | \mathbf{H}_l | x_{n_m} \rangle_{G_l} = |\Pi_l^{-1}(n)| \langle x | \mathbf{H}_l | x \rangle_{G_l} = H_l(x, x)$$

where the last equality holds as  $|\Pi_l^{-1}(n)|$  cancels the weights in the inner product defined on  $G_l$ . Similar reasoning will give the second part of the statement. Assume  $y$  is adjacent to  $x$  such that  $y \in \Pi_l^{-1}(n+1) = \{y_{n_1}, \dots, y_{n_k}\}$ ,

$$\begin{aligned} \langle \Pi_l(x) | \mathbf{J}_l | \Pi_l(x) + 1 \rangle_l &= \langle P_l^* \Pi_l(x) | \mathbf{H}_l | P_l^* (\Pi_l(x) + 1) \rangle_{G_l} \\ &= (\langle x_{n_1} | + \cdots + \langle x_{n_m} |) \mathbf{H}_l (|y_{n_1}\rangle + \cdots + |y_{n_k}\rangle) \\ &= \mathbf{deg}_+(x) |\Pi_l^{-1}(n)| \langle x | \mathbf{H}_l | y \rangle_{G_l} \\ &= \mathbf{deg}_+(x) H_l(x, y) \end{aligned}$$

To prove the third statement, we first observe that the previous computations verify the following equation,

$$\langle \Pi_l(x) | \mathbf{J}_l | \Pi_l(x) + 1 \rangle_l = \mathbf{deg}_+(x) |\Pi_l^{-1}(n)| \langle x | \mathbf{H}_l | y \rangle_{G_l}$$

Similarly, we can show

$$\langle \Pi_l(x) + 1 | \mathbf{J}_l | \Pi_l(x) \rangle_l = \mathbf{deg}_-(y) |\Pi_l^{-1}(n+1)| \langle y | \mathbf{H}_l | x \rangle_{G_l}.$$

Hence, it suffices to prove  $\mathbf{deg}_-(y) |\Pi_l^{-1}(n+1)| = \mathbf{deg}_+(x) |\Pi_l^{-1}(n)|$ . The last equality holds as both left-hand side and the right-hand side give the number of edges between the transversal layers  $\Pi_l^{-1}(n)$  and  $\Pi_l^{-1}(n+1)$ .

**Proof of Theorem 1** We observe

$$(\mathbf{J}_l)^k = P_l \mathbf{H}_l P_l^* \cdot P_l \mathbf{H}_l P_l^* \cdots P_l \mathbf{H}_l P_l^* = P_l (\mathbf{H}_l \mathbf{Proj}_l)^k P_l^*$$

where  $P_l^* = \mathbf{Proj}_l P_l^*$  holds due to Lemma 3 and  $P_l^* P_l = \mathbf{Proj}_l$  due to Lemma 5. Hence,

$$P_l e^{i T_l \mathbf{H}_l \mathbf{Proj}_l} P_l^* |0\rangle = P_l e^{i\phi} P_l^* |N\rangle \Rightarrow P_l e^{i T_l \mathbf{H}_l \mathbf{Proj}_l} |x_L\rangle = P_l e^{i\phi} |x_R\rangle$$

which implies  $e^{i T_l \mathbf{H}_l \mathbf{Proj}_l} |x_L\rangle - e^{i\phi} |x_R\rangle \in \text{Ker}(P_l)$ . Note that  $|x_L\rangle = P_l^* |0\rangle$  and  $|x_R\rangle = P_l^* |N\rangle$ . By Corollary 4 and by the fact that  $|x_L\rangle, |x_R\rangle \in L^2_{\text{sym}}(G_l)$ , we conclude

$$e^{i T_l \mathbf{H}_l \mathbf{Proj}_l} |x_L\rangle = e^{i\phi} |x_R\rangle$$

Let  $\mathbf{Proj}_l^\perp$  be the projection of  $L^2(G_l)$  onto  $(L^2_{\text{sym}}(G_l))^\perp$ . We observe

$$(\mathbf{H}_l \mathbf{Proj}_l + \mathbf{H}_l \mathbf{Proj}_l^\perp) |x_L\rangle = \mathbf{H}_l \mathbf{Proj}_l |x_L\rangle,$$

which implies  $e^{i T_l \mathbf{H}_l} |x_L\rangle = e^{i\phi} |x_R\rangle$ .

## 5 Conclusions and outlook

Our construction provides an infinite set of new examples of novel geometries for which perfect quantum state transfer can be achieved. For example, using the spin coupling values  $J_n$  in (4) for the simplest case of a spin chain, combined with our Hamiltonian construction in Proposition 1 and Theorem 1, we find perfect quantum state transfer on diamond fractals such as those shown in Figs. 1 and 2. This clearly generalizes to the set of quantum systems on the graphs  $G_l$  described in Sect. 3. The basic projection idea is very general and applicable to many other fractal-type graphs, which allows to construct further examples. This opens up the possibility to *design* perfect quantum state transfer on fractal-like structures with special features. The existence of the results for Green's functions for these structures means that other quantum information properties such as fidelity and entanglement can be studied for these fractal structures. Moreover, our approach allows to consider other transport phenomena involving linear and nonlinear, classical and quantum waves on certain graphs, quantum graphs, and fractals. This will be the subject of future research [44].

**Acknowledgements** This research was supported in part by the University of Connecticut Research Excellence Program, by DOE Grant DE-SC0010339 and by NSF Grants 1613025 and 2008844. The authors are grateful to Eric Akkermans, Patricia Alonso-Ruiz, and Gabor Lippner for interesting and helpful discussions. The authors are grateful to anonymous referees for suggested improvements to the paper.

## References

1. Bose, S.: Quantum communication through an unmodulated spin chain. *Phys. Rev. Lett.* **91**(20), 207901 (2003)
2. Bose, S.: Quantum communication through spin chain dynamics: an introductory overview. *Contemp. Phys.* **48**, 13–30 (2007)
3. Kay, A.: A review of perfect state transfer and its applications as a constructive tool. *Int. J. Quantum Inform.* **641**(8). Preprint quant-ph/0903.4274 (2010)
4. Christandl, M., Vinet, L., Zhedanov, A.: Analytic next-to-nearest-neighbor  $x$   $x$  models with perfect state transfer and fractional revival. *Phys. Rev. A* **96**(3), 032335 (2017)
5. Kempton, M., Lippner, G., Yau, S.-T.: Perfect state transfer on graphs with a potential. *Quantum Inf. Comput.* **17**(3–4), 303–327 (2017)
6. Christandl, M., Datta, N., Ekert, A., Landahl, A.J.: Perfect state transfer in quantum spin networks. *Phys. Rev. Lett.* **92**(18), 187902 (2004)
7. Burgarth, D., Bose, S.: Conclusive and arbitrarily perfect quantum-state transfer using parallel spin-chain channels. *Phys. Rev. A* **71**(5), 052315 (2005)
8. Burgarth, D., Bose, S.: Perfect quantum state transfer with randomly coupled quantum chains. *New J. Phys.* **7**(1), 135 (2005)
9. Karbach, P., Stolze, J.: Spin chains as perfect quantum state mirrors. *Phys. Rev. A* **72**(3), 030301 (2005)
10. Angeles-Canul, R.J., Norton, R.M., Opperman, M.C., Paribello, C.C., Russell, M.C., Tamon, C.: Perfect state transfer, integral circulants, and join of graphs. *Quantum Inf. Comput.* **10**(3–4), 325–342 (2010)
11. Bachman, R., Fredette, E., Fuller, J., Landry, M., Opperman, M., Tamon, C., Tollefson, A.: Perfect state transfer on quotient graphs. *Quantum Inf. Comput.* **12**(3–4), 293–313 (2012)
12. Godsil, C.: When can perfect state transfer occur? *Electron. J. Linear Algebra* **23**, 877–890 (2012)
13. Bernasconi, A., Godsil, C., Severini, S.: Quantum networks on cubelike graphs. *Phys. Rev. A* **(3)** **78**(5), 052320 (2008)
14. Godsil, C.: State transfer on graphs. *Discrete Math.* **312**(1), 129–147 (2012)
15. Vinet, L., Zhedanov, A.: Para-Krawtchouk polynomials on a bi-lattice and a quantum spin chain with perfect state transfer. *J. Phys. A* **45**(26), 265304 (2012)

16. Qin, W., Wang, C., Long, G.L.: High-dimensional quantum state transfer through a quantum spin chain. *Phys. Rev. A* **87**(1), 012339 (2013)
17. Kempton, M., Lippner, G., Yau, S.-T.: Pretty good quantum state transfer in symmetric spin networks via magnetic field. *Quantum Inf. Process.* **16**(9), 210 (2017)
18. Kirkland, S., McLaren, D., Pereira, R., Plosker, S., Zhang, X.: Perfect quantum state transfer in weighted paths with potentials (loops) using orthogonal polynomials. *Linear Multilinear Algebra* **67**(5), 1043–1061 (2019)
19. Vinet, L., Zhedanov, A.: How to construct spin chains with perfect state transfer. *Phys. Rev. A* **85**(1), 012323 (2012)
20. Berker, A.N., Ostlund, S.: Renormalisation-group calculations of finite systems: order parameter and specific heat for epitaxial ordering. *J. Phys. C Solid State Phys.* **12**(22), 4961 (1979)
21. Griffiths, R.B., Kaufman, M.: Spin systems on hierarchical lattices. Introduction and thermodynamic limit. *Phys. Rev. B* **26**(9), 5022 (1982)
22. Kaufman, M., Griffiths, R.B.: Spin systems on hierarchical lattices. II. Some examples of soluble models. *Phys. Rev. B* **30**(1), 244 (1984)
23. Malozemov, L., Teplyaev, A.: Pure point spectrum of the Laplacians on fractal graphs. *J. Funct. Anal.* **129**(2), 390–405 (1995)
24. Akkermans, E., Dunne, G., Teplyaev, A.: Physical consequences of complex dimensions of fractals. *EPL* **88**(4), 40007 (2009)
25. Hambly, B.M., Kumagai, T.: Diffusion on the scaling limit of the critical percolation cluster in the diamond hierarchical lattice. *Commun. Math. Phys.* **295**(1), 29–69 (2010)
26. Barlow, M.T., Evans, S.N.: Markov processes on vermiculated spaces. In: Kaimanovich, V.A. (ed.) *Random walks and geometry. Proceedings of the workshop held in Vienna, June 18–July 13, 2001. In collaboration with Klaus Schmidt and Wolfgang Woess*. Walter de Gruyter GmbH & Co. KG, Berlin. ISBN: 3-11-017237-2 (2004)
27. Nekrashevych, V., Teplyaev, A.: Groups and analysis on fractals. In: *Analysis on Graphs and Its Applications*, Volume 77 of *Proceedings of the Symposium Pure Mathematical*. American Mathematical Society, Providence, pp. 143–180 (2008)
28. Patricia Alonso Ruiz: Explicit formulas for heat kernels on diamond fractals. *Commun. Math. Phys.* **364**(3), 1305–1326 (2018)
29. Alonso Ruiz, P.: Heat kernel analysis on diamond fractals. [arXiv:1906.06215](https://arxiv.org/abs/1906.06215) (2019)
30. Teplyaev, A.: Harmonic coordinates on fractals with finitely ramified cell structure. *Can. J. Math.* **60**(2), 457–480 (2008)
31. Malozemov, L., Teplyaev, A.: Self-similarity, operators and dynamics. *Math. Phys. Anal. Geom.* **6**(3), 201–218 (2003)
32. Brzoska, A., Coffey, A., Hansalik, M., Loew, S., Rogers, L.G.: Spectra of magnetic operators on the diamond lattice fractal. [arXiv:1704.01609](https://arxiv.org/abs/1704.01609) (2017)
33. Alonso-Ruiz, P., Hinz, M., Teplyaev, A., Treviño, R.: Canonical diffusions on the pattern spaces of aperiodic delone sets. [arXiv:1801.08956](https://arxiv.org/abs/1801.08956) (2018)
34. Steinhurst, B., Teplyaev, A.: Spectral analysis and Dirichlet forms on Barlow-Evans fractals. *J. Spectr. Theory*, to appear (2020). [arXiv:1204.5207](https://arxiv.org/abs/1204.5207)
35. Bajorin, N., Chen, T., Dagan, A., Emmons, C., Hussein, M., Khalil, M., Mody, P., Steinhurst, B., Teplyaev, A.: Vibration modes of  $3n$ -gaskets and other fractals. *J. Phys. A* **41**(1), 015101 (2008)
36. Bajorin, N., Chen, T., Dagan, A., Emmons, C., Hussein, M., Khalil, M., Mody, P., Steinhurst, B., Teplyaev, A.: Vibration spectra of finitely ramified, symmetric fractals. *Fractals* **16**(3), 243–258 (2008)
37. Akkermans, E., Dunne, G.V., Teplyaev, A.: Thermodynamics of photons on fractals. *Phys. Rev. Lett.* **105**(23), 230407 (2010)
38. Akkermans, E., Benichou, O., Dunne, G.V., Teplyaev, A., Voituriez, R.: Spatial log-periodic oscillations of first-passage observables in fractals. *Phys. Rev. E* **86**(6), 061125 (2012)
39. Akkermans, E., Chen, J.P., Dunne, G., Rogers, L.G., Teplyaev, A.: Fractal AC circuits and propagating waves on fractals. In: *6th Cornell Fractals Conference Proceedings, Analysis, Probability and Mathematical Physics on Fractals*, Chapter 18, pp. 557–567 (2020). [arXiv:1507.05682](https://arxiv.org/abs/1507.05682)
40. Akkermans, E.: Statistical mechanics and quantum fields on fractals. In: Carfi, D., Lapidus, M.L., Pearse, E.P.J., van Frankenhuijsen, M. (eds.) *Fractal Geometry and Dynamical Systems in Pure and Applied Mathematics. II. Fractals in Applied Mathematics*, Contemporary Mathematics, vol. 601. American Mathematical Society, Providence, RI. ISBN: 978-0-8218-9148-3 (2013)
41. Dunne, G.V.: Heat kernels and zeta functions on fractals. *J. Phys. A* **45**(37), 374016 (2012)

42. Alonso-Ruiz, P., Kelleher, D.J., Teplyaev, A.: Energy and Laplacian on Hanoi-type fractal quantum graphs. *J. Phys. A* **49**(16), 165206 (2016)
43. Hinz, M., Meinert, M.: On the viscous Burgers equation on metric graphs and fractals. *J. Fractal Geom.* **7**(2), 137–182 (2020)
44. Mograby, G., Derevyagin, M., Dunne, G.V., Teplyaev, A.: Spectra of perfect state transfer Hamiltonians on fractal-like graphs. [arXiv:2003.11190](https://arxiv.org/abs/2003.11190) (2020)
45. Mograby, G., Derevyagin, M., Dunne, G.V., Teplyaev, A.: Hamiltonian systems, Toda lattices, solitons, Lax pairs on weighted  $\mathbb{Z}$ -graded graphs. [arXiv:2008.04897](https://arxiv.org/abs/2008.04897) (2020)
46. Krön, B., Teufel, E.: Asymptotics of the transition probabilities of the simple random walk on self-similar graphs. *Trans. Am. Math. Soc.* **356**(1), 393–414 (2004)
47. Lang, U., Plaut, C.: Bilipschitz embeddings of metric spaces into space forms. *Geom. Dedicata* **87**(1–3), 285–307 (2001)
48. Szegő, G.: *Orthogonal Polynomials*. Colloquium Publications, vol. XXIII, 4th edn. American Mathematical Society, Providence (1975)

**Publisher's Note** Springer Nature remains neutral with regard to jurisdictional claims in published maps and institutional affiliations.